



Hand Guidance Using Grasping Metaphor and Wearable Haptics

Tommaso Lisini Baldi, Nicole d'Aurizio, Domenico Prattichizzo

► To cite this version:

Tommaso Lisini Baldi, Nicole d'Aurizio, Domenico Prattichizzo. Hand Guidance Using Grasping Metaphor and Wearable Haptics. IEEE Haptics Symposium (HAPTICS), Mar 2020, Washington, United States. hal-02550431

HAL Id: hal-02550431

<https://hal.science/hal-02550431>

Submitted on 22 Apr 2020

HAL is a multi-disciplinary open access archive for the deposit and dissemination of scientific research documents, whether they are published or not. The documents may come from teaching and research institutions in France or abroad, or from public or private research centers.

L'archive ouverte pluridisciplinaire **HAL**, est destinée au dépôt et à la diffusion de documents scientifiques de niveau recherche, publiés ou non, émanant des établissements d'enseignement et de recherche français ou étrangers, des laboratoires publics ou privés.

Hand Guidance Using Grasping Metaphor and Wearable Haptics

Tommaso Lisini Baldi¹, Nicole D’Aurizio^{1,2}, and Domenico Prattichizzo^{1,2}

Abstract—In this work, we propose a novel method for hand guidance, combining grasping metaphor and wearable haptics. To guide the hand towards the desired orientation, the system generates vibrations exploiting the grasp theory, asking the user to align the perceived wrench with the gravity. To evaluate the system and demonstrate its potentiality, different vibrotactile feedback approaches have been tested. Both constant and error-dependent vibration intensities were considered as feedback methods. Experimental results confirmed the capability of the proposed approach in guiding the hand of the users towards target orientations in a limited time with high accuracy. Users’ experience feedback, supported by the statistical analysis of the data, shows that providing information about the actual orientation error is crucial to accomplish the task in minor time.

I. INTRODUCTION

Haptic devices capable of providing cutaneous stimuli have recently gained attention in the haptics and robotics research fields. Several researchers have developed and exploited such technologies in contexts like teleoperation and navigation, demonstrating how promising they are. As a matter of fact, cutaneous feedback not only is able to enhance the potentiality of augmented reality [1], but also provides an effective way to simplify the device design, allowing to reduce the form factor to make them more wearable and lightweight [2]. In addition to tasks involving cutaneous sensation, wearable haptics is widely used for navigation and body guidance purposes. In [3] and [4] authors have already documented the efficiency of suggesting both cadence and directions during the walk, while in [5] the potentiality of haptics in guiding a part of the body is demonstrated. In fact, thanks to its versatility, cutaneous stimulation can be useful for a wide range of applications. Examples include training [6], motor skills teaching tasks [7], teleoperation [8], and virtual reality [9], [10]. Moreover, the valid alternative that haptic feedback can offer to visual or audio signals should not be underestimated. Not always those sensory channels are available, indeed they could be overloaded or unusable due to task requirements, environmental factors, vision or hearing impairments. This can be experienced in circumstances as surgeons requiring fine-grained guidance for complex maneuvers [11], rescuers needing suggestions in rooms with poor visibility due to smoke or dust [12],



Fig. 1: Haptic hand guidance using vibrations in a demonstrative Virtual Reality scenario. The user wears the haptic thimbles and orients the hand following the cues displayed at the user’s finger pulps. The fingertips and the palm positions are tracked by a Leap Motion device placed on the table.

operators desiring to know in advance the best way to approach a tool.

As far as it concerns position and orientation of the human hand, many studies have been conducted on hand guidance by means of wearable haptic devices. In this aim, pseudo-attraction force [13], torque stimulus [14], shape-changing effect [15], skin stretch [16], and vibrations [5] are the most widespread haptic technologies. The majority of the aforementioned methods mainly rely on hand-held devices or make use of cues displayed in other body parts (e.g., wrist, arm, forearms, etc.). As an example, in [13] the user experiences a kinesthetic illusion characterized by the sensation of being continuously pushed or pulled by the device. Similarly, Walker *et al.* in [14] exploit ungrounded haptic feedback by spinning and rotating flywheels. This produces a moment pulse proportional to the spin and to the rotation speed. In [15] the authors designed a shape-changing hand-held device to provide pedestrian navigation instructions. The device resembled a cube with an upper half that rotates and translates with respect to the bottom half. The pose corresponds to heading and proximity to the target. Furthermore, another group of cutaneous devices providing orientation information takes advantage of skin stretch stimuli. These devices exploit the high sensitivity of human skin to tangential stretches, providing the human user with rich directional information. For instance, Chinello *et*

¹Tommaso Lisini Baldi, Nicole D’Aurizio, and Domenico Prattichizzo are with the Department of Information Engineering and Mathematics, University of Siena, Via Roma 56, I-53100 Siena, Italy. {lisini, ndaurizio, prattichizzo}@diism.unisi.it

²Nicole D’Aurizio and Domenico Prattichizzo are with the Department of Advanced Robotics, Istituto Italiano di Tecnologia, Genova, 16163, Italy. {nicole.daurizio, domenico.prattichizzo}@iit.it

al. in [16] present a portable unobtrusive device for the forearm that can generate independent skin stretch stimuli encoding different hand orientation patterns. In addition to the foregoing techniques, there is an increasing interest in vibrotactile cutaneous feedback. The compact and lightweight form factor of eccentric mass motors has, in fact, empowered researchers to design highly wearable vibrotactile interfaces. For example, Aggravi *et al.* in [5] describe a possible solution to let a robot guide the position of a human operator's hand by using a vibrotactile armband. In [17] the authors use two vibrotactile motors (placed either on the palm or on the back of the hand) to suggest directional information.

The main novelty introduced in this paper is a guidance approach implementing the paradigm “*what you feel what you do*”. Indeed, the purpose of the *interface metaphor* is to give the user instantaneous knowledge about how to interact with the interface, provided that it is designed to be similar to physical entities [18]. We take advantage of haptic thimbles with a single vibro-motor. The idea is to use a combination of vibrations to suggest human hand motion. To guide the hand towards a desired orientation, the system exploits the illusion of grasping a virtual object. The user has to orient the wrench generated by the object weight until it is aligned with the gravity (Figure 1). The use of vibrations for force rendering and interaction with virtual objects has already been studied and tested [19].

The proposed framework has been evaluated with eight subjects evaluating two different guidance policies. In the former the intensity of the motor vibration remained constant, whereas in the latter the intensity of the vibration was regulated in accordance with the orientation error. To prove the reliability and accuracy of guiding on the basis of vibrating thimbles, we use a high precision external camera-based tracking system. To the best of our knowledge, this represents the first attempt to guide the human hand using wearable haptic thimbles and grasping metaphor.

II. HAPTIC GUIDANCE SYSTEM

In the previous section, we introduced the problem and briefly outlined and discussed the state of the art. In what follows we describe the novelty of our system and its implementation.

A. System description

With the aim to provide the user with an immediate knowledge on how to interact with the proposed system, the guidance policy here described implements an interface metaphor based on the way humans grasp objects. To begin with, it is useful to briefly review some notion mentioned here. By definition, a wrench \mathbf{w} is a combination of a couple with a force along its axis. Moreover, we will refer to the forces applied at the contact points as *contact forces* \mathbf{F} . For the purposes of the developed method, unless otherwise specified, following wrenches will be expressed with respect to the object reference frame, while each contact force will be expressed with respect to the correspondent contact point reference frame. An object grasped with k contacts points is

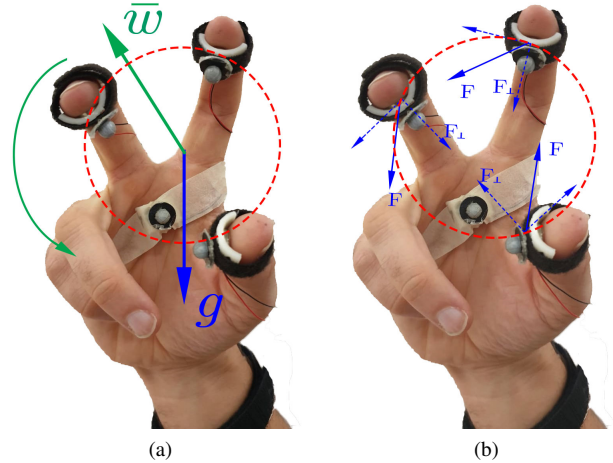


Fig. 2: Users are tasked to rotate the hand aligning the wrench $\bar{\mathbf{w}}$ generated by the virtual object (red dashed circle) with the gravity \mathbf{g} . The contact points position (b) is estimated using a high precision tracking system. We tested two situations in which three and four contact points are involved in the grasp. For each scenario, four different modalities were evaluated: *i*) contact force and variable intensity ($\mathbf{F}+\mathbf{V}$); *ii*) normal contact force component and variable intensity ($\mathbf{F}_\perp+\mathbf{V}$); *iii*) contact force and constant intensity ($\mathbf{F}+\mathbf{C}$); *iv*) normal contact force component and constant intensity ($\mathbf{F}_\perp+\mathbf{C}$).

in equilibrium when the sum of the forces applied to is zero, *i.e.*,

$$\sum_{i=1}^k {}^O\mathbf{F}_i + \mathbf{w} = 0$$

where ${}^O\mathbf{F}_i$ is the i -th contact force expressed in object reference frame. Moreover, the force and moment balance for the object can be described by the equation

$$\mathbf{w} = -\mathbf{G}\lambda, \quad \mathbf{w} \in \mathbb{R}^n, \quad \lambda \in \mathbb{R}^m, \quad \mathbf{G} \in \mathbb{R}^{n \times m} \quad (1)$$

where $n=6$ for the general three dimensional case, λ is the contact force vector with $m=3k$ for k contact points, \mathbf{G} is the grasp matrix. The interested reader is referred to [20].

The innovative technique here presented is thought to guide the orientation of the hand by taking advantage of a wrench representing the weight of an ideal object seized by the user, as depicted in Figure 2a. Following the grasping metaphor, the mental connection between the two forces suggests that the target orientation is reached once the perceived wrench is aligned to the gravity. Since a real object generates forces on the contact points, to induce the same perception it is necessary to know how to generate equivalent contact forces.

As starting point, the actual posture of the user's hand is associated with k contact points ($\mathbf{C}_1, \mathbf{C}_2, \dots, \mathbf{C}_k \in \mathbb{R}^3$) (Figure 2b). Once the identification is done, it is possible to apply an external force to the virtual object inscribed within

the contact points and ask the subject to align this force with the gravity. With this aim, it is necessary to define the object center of gravity \mathbf{O} as

$$\mathbf{O}_j = \frac{\sum_{i=1}^k C_{j,i}}{k}, \quad \mathbf{O} \in \mathbb{R}^3.$$

Once the object reference frame Σ_O is set, each contact point reference frame Σ_i , $i = 1, \dots, k$, can be defined with the y_i axis on the direction of the vector $\overline{\mathbf{OC}_i}$ and the x_i axis on the direction of the cross-product of the latter and the y_O axis. The rotation matrices describing the orientation of each Σ_i with respect to Σ_O can be expressed by the Rodrigues' Formula as

$$\mathbf{R}_i = \mathbf{I} + (\sin\theta_i)\mathbf{K}_i + (1 - \cos\theta_i)\mathbf{K}_i^2, \quad i = 1, \dots, k$$

where θ_i is the angle between y_O and y_i , and \mathbf{K}_i is the cross-product matrix for the unit vector x_i . Thus, the grasp matrix \mathbf{G} can be modeled as

$$\mathbf{G} = [\mathbf{G}_1^T \ \mathbf{G}_2^T \ \dots \ \mathbf{G}_k^T], \quad \mathbf{G}^T \in \mathbb{R}^{6k \times 6}$$

being

$$\mathbf{G}_i^T = \mathbf{R}_i \begin{bmatrix} \mathbf{I}_{3 \times 3} & -\mathbf{S}_i \\ 0 & \mathbf{I}_{3 \times 3} \end{bmatrix}, \quad \mathbf{G}_i^T \in \mathbb{R}^{6 \times 6}$$

where \mathbf{S}_i is the cross-product matrix of the vector $\overline{\mathbf{C}_i\mathbf{O}}$.

As a result, it is possible to map the object twist into the contact frames,

$$\mathbf{w} = -\tilde{\mathbf{G}}\lambda$$

where

$$\begin{aligned} \tilde{\mathbf{G}}^T &= \mathbf{H}\mathbf{G}^T, \\ \mathbf{w} &= [f_{Ox} \ f_{Oy} \ f_{Oz} \ m_{Ox} \ m_{Oy} \ m_{Oz}]^T \in \mathbb{R}^6, \\ \lambda &= [\lambda_1 \ \lambda_2 \ \dots \ \lambda_k]^T \in \mathbb{R}^{3k}, \end{aligned}$$

and

$$\lambda_i = \mathbf{H}_i [f_{ix} \ f_{iy} \ f_{iz} \ m_{ix} \ m_{iy} \ m_{iz}]^T \in \mathbb{R}^3.$$

Accordingly with [20], we assumed a hard-finger (HF) contact model for each point, thus the selection matrix \mathbf{H} can be defined as

$$\mathbf{H} = \text{Blockdiag}(\mathbf{H}_1, \dots, \mathbf{H}_k) \in \mathbb{R}^{3k \times 6k}$$

with

$$\mathbf{H}_i = [\mathbf{I}_{3 \times 3} \ \mathbf{0}_{3 \times 3}] \in \mathbb{R}^{3 \times 6}.$$

Since the grasp here modeled is virtual, as starting condition it can be assumed that the object is at the static force equilibrium condition. It follows that it is possible to apply an external wrench $\bar{\mathbf{w}}$ to the object and compute the contact force components $\bar{\lambda}$ that are transmitted through the contact points to maintain the equilibrium. Starting from (1), we obtain

$$\bar{\mathbf{w}} + \tilde{\mathbf{G}}\bar{\lambda} = 0$$

Algorithm 1

Input: $\mathbf{C}_1, \mathbf{C}_2, \dots, \mathbf{C}_k \in \mathbb{R}^3 \ \bar{\mathbf{w}} \in \mathbb{R}^{6 \times 1}$

Output: $m_i \ i = 1, \dots, k$

```

 $\mathbf{O} = \frac{\sum_{i=1}^k \mathbf{C}_i}{k}$ 
for  $i = 1, \dots, k$  do
     $\mathbf{y}_i = \overline{\mathbf{OC}_i}$ 
     $\mathbf{x}_i = \mathbf{y}_i \times \mathbf{y}_O$ 
     $\mathbf{z}_i = \mathbf{y}_i \times \mathbf{x}_i$ 
     $\mathbf{R}_i = \mathbf{I} + (\sin\theta_i)\mathbf{K}_i + (1 - \cos\theta_i)\mathbf{K}_i^2$ 
     $\mathbf{G}_i^T = \mathbf{R}_i \begin{bmatrix} \mathbf{I}_{3 \times 3} & -\mathbf{S}_i \\ \mathbf{0}_{3 \times 3} & \mathbf{I}_{3 \times 3} \end{bmatrix}$ 
end for
 $\mathbf{G} = [\mathbf{G}_1^T \ \dots \ \mathbf{G}_k^T]$ 
 $\tilde{\mathbf{G}}^T = \mathbf{H}\mathbf{G}^T$ 
 $\bar{\lambda} = -\tilde{\mathbf{G}}^\dagger \bar{\mathbf{w}} + N(\tilde{\mathbf{G}})\xi$ 
if  $\mathbf{y}_i \cdot \bar{\mathbf{w}} \leq 0$  then
     $\lambda_{des_i} = \lambda_i$ 
else
     $\lambda_{des_i} = [0 \ 0 \ 0]^T$ 
end if
GetBestSolution  $\min_{\xi} ||\lambda_{des} - \bar{\lambda}||$ 
s.t.:
 $\bar{\lambda}_{ix} \geq 0, \ \bar{\lambda}_{iy} \geq 0, \ \bar{\lambda}_{iz} \geq 0 \quad i = 1, \dots, k$ 
 $\lambda^* = \frac{\lambda + N(\tilde{\mathbf{G}})\xi}{||\lambda + N(\tilde{\mathbf{G}})\xi||}$ 
for  $i = 1, \dots, k$  do
    if Feedback =  $\mathbf{F}_\perp$  then
         $m_i = \lambda_{iy}^*$ 
    else if Feedback =  $\mathbf{F}$  then
         $m_i = ||\lambda_i^*||$ 
    end if
    if Mode =  $\mathbf{C}$  then
         $m_i = f(\frac{m}{||m||})$ 
    if Mode =  $\mathbf{V}$  then
         $m_i = \alpha \cdot f(\frac{m}{||m||})$ 
    end if
end for

```

that implies

$$\bar{\lambda} = -\tilde{\mathbf{G}}^\dagger \bar{\mathbf{w}} + N(\tilde{\mathbf{G}})\xi$$

where $\tilde{\mathbf{G}}^\dagger$ is the pseudoinverse of the matrix $\tilde{\mathbf{G}}$, $N(\tilde{\mathbf{G}})$ indicates a matrix whose columns form a basis for $\mathcal{N}(\tilde{\mathbf{G}})$ ¹ while ξ is a vector chosen to optimize $\bar{\lambda}$, as detailed below. Indeed, since $\bar{\lambda}$ is mapped in the vibration motors placed at the contact points, it is not desirable to have values $\bar{\lambda}_i < 0$. Therefore, the term $N(\tilde{\mathbf{G}})\xi$ can be used to manipulate $\bar{\lambda}$ so that the information the subject can retrieve from the haptic

¹ $\mathcal{N}(A)$ indicates the null space of matrix A .

feedback is maximized, *i.e.* $\bar{\lambda}_i > 0 \forall i$. To this goal, all the contact points that can apply a positive force are selected as relevant, considering

$$C_i = \begin{cases} 1 & \text{if } [\bar{w}_1 \ \bar{w}_2 \ \bar{w}_3] \cdot \overline{OC_i}^T \leq 0 \\ 0 & \text{otherwise.} \end{cases}$$

It is worth pointing out that by definition of the object's center of gravity, there is no case in which all the C_i are 0.

To define the desired haptic feedback, firstly, the vector $\lambda_{des} \in \mathbb{R}^{3k}$ is composed as follows:

$$\lambda_{des_i} = C_i \bar{\lambda}_i$$

and secondly, it is normalized. The optimal solution ξ^* , chosen in accordance with [21], is the one that minimizes the difference between λ_{des} and $\bar{\lambda}$, *i.e.*,

$$\begin{aligned} \min_{\xi} \quad & \|\lambda_{des} - \bar{\lambda}(\xi)\| \\ \text{s.t.} \quad & \bar{\lambda}(\xi)_i = [\bar{f}_{ix} \ \bar{f}_{iy} \ \bar{f}_{iz}]^T \geq 0. \end{aligned} \quad (2)$$

Although it is implicit in the current formulation, we stress that the problem (2) is a Quadratic Programming (QP) problem, under the condition $N^T(G) \cdot N(G)$ is positive semi-definite. QP is a class of convex problems for which several efficient algorithms exist in literature making possible to solve them online with a contained computational burden [22].

Consequently, the optimal set of contact forces results

$$\bar{\lambda}^* = -\tilde{\mathbf{G}}^\dagger \tilde{\mathbf{w}} + N(\tilde{\mathbf{G}})\xi^*.$$

The computed $\bar{\lambda}^*$ is the vector used to drive the motors. Two policies were tested within this work:

- 1) the intensity of the motors depends on the norm of the contact force (F);
- 2) the intensity of the motors is related only to the normal component of each contact force (F_\perp).

Each approach was tested in a twofold manners: adjusting the intensity of the motor on the basis of the orientation error and maintaining it constant till the goal is reached.

B. Hardware Implementation

To suggest the hand orientation, we provide vibrotactile stimuli via haptic thimbles. The system consists of four thimbles, an Arduino Pro-mini 3.3V, a 3.7V Li-Po battery, and a RN-42 Bluetooth antenna. Each thimble is made by ABS and contains a small coin-factor eccentric mass motor (Precision Microdrives Model 310-103 [23]). The electronic components and the battery are embedded into a 3D printed case. The Bluetooth baudrate for the communication is 115200 bps. Motors are controlled using the PWN output pins, where the maximum voltage (3.3 V) corresponds to a PWM value of 255, whereas the minimum of 0.9 V corresponds to 70. In Figure 3 a thimble and an user wearing it are depicted.



Fig. 3: The vibrotactile cutaneous thimble. A vibromotor (A) is enclosed on a 3D printed thimble (B). A Velcro® belt (C) enables the user to easily fasten the device on the finger. The total weight of the thimble is 3.02 g.

III. EXPERIMENTAL VALIDATION

In this section we describe the experimental validation conducted to assess the capability of the system in guiding the hand. The two feedback strategies (F and F_\perp) described in Section II have been tested exploiting two different modalities. In the first case, the system was set up to stop the vibration only once the desired orientation was reached and maintained for at least 0.5 s. In the latter, the intensity of vibration was modulated proportionally to the orientation error. We refer to them as *constant* intensity (C) and *varying* intensity (V), respectively.

To evaluate the real capability of the system in guiding the users' hand, an experimental validation has been conducted on 8 subjects (2 females and 6 males, aged between 23 and 54). All subjects were right-handed. Six subjects had no experience with vibrotactile interfaces and haptics, one subject had limited experience and one subject had extensive experience. None of them reported any known deficiencies in perception abilities or physical impairments. An introduction of the experiment and training for the system handling was given to each participant. Subjects were asked to sign informed consent documents and were able to discontinue participation at any time. The experimental evaluation protocol followed the Declaration of Helsinki. The total time of the experiments for each participant did not exceed thirty minutes.

A set of 12 wrenches were pseudo-randomly generated in order to have 5 wrenches involving single motor vibration and 7 wrenches resulting in a combination of multiple motors. The 8 participants, randomly labeled from U1 to U8 for convenience, were tasked to orient the hand following the haptic cueing, *i.e.*, to align the virtual wrench with the gravity. Even if the system is compatible with multiple tracking systems, a Vicon system was used as a ground truth in the experimental validation to track the users' hand configuration and to record the time needed to accomplish the task. Retroreflective markers were positioned on fingertips and palm as depicted in Figure 2. A familiarization period of 2 minutes was provided to participants to acquaint them with the system. To test the users capability in orienting

a virtual object on the basis of the haptic feedback, two different grasp configurations were proposed. In the first case, three contact points were positioned on the fingertip of thumb, index finger, and middle finger. In the second one a fourth contact point was added and located on the palm, approximately between the first and second knuckle. Both configurations were tested using the same wrench set.

Participants to the validation campaign were involved in both settings. They tested the following feedback-modalities combinations randomly ordered: contact force and variable intensity (F+V), normal contact force component and variable intensity (F_⊥+V), contact force and constant intensity (F+C), normal contact force component and constant intensity (F_⊥+C). For all the trials, a threshold of 3° for the axes alignment was set to discard potential hand tremors [24]. Each attempt lasted maximum 90s, beyond which the test was interrupted and 90 was reported as elapsed time. At the end of each session of trials, a NASA Task Load Index questionnaire [25] was proposed to the participant, with the aim of assessing the perceived load in term of Mental Demand (MD), Temporal Demand (TD), Physical Demand (PD), Performance (PE), Effort (EF), and Frustration (FR). This method assesses work load on a 7-point scales. Each of the six questions has a scale of 21 levels, considering 1 as “very low” and 21 as “very high”. Results of the survey are reported in Table III.

A. Constant Vibration Intensity (C)

The purpose of this setup was to evaluate the capability in orienting the hand when no information about the error is provided.

As reported in Algorithm 1, the value assumed by each motor depends only on the computed λ^* and it remains constant until the target position is reached. In particular, in case of F_⊥-policy,

$$m_i = \lambda_{i_y}^* \quad i = 1, \dots, k \quad (3)$$

where m_i is the motor reference value, and $\lambda_{i_y}^*$ is the normal component associated to the i -th contact point. For what concerns the F-policy,

$$m_i = \|\lambda_i^*\| \quad i = 1, \dots, k \quad (4)$$

i.e. all the three components of λ_i^* are taken into account for the i -th contact point. In both cases, the obtained vector may have non-unitary norm, so that a normalization is needed

$$\mathbf{m} = \frac{\mathbf{m}}{\|\mathbf{m}\|}. \quad (5)$$

Finally, the PWM value of the i -th motor at each time t is obtained in accordance with [23] as

$$m_i(t) = \begin{cases} 70 + |m_i| \cdot 185 & \text{if } |m_i| > 0 \\ 0 & \text{otherwise.} \end{cases}$$

The trial ends when the error in orientation remains under the threshold for at least 0.5s.

Participants performed the test both modeling the grasping with three and four contact points. Results and discussion are reported in the next section.

3 Contact Points					4 contact Points			
Modality	F+V	F _⊥ +V	F+C	F _⊥ +C	F+V	F _⊥ +V	F+C	F _⊥ +C
Successes	96	96	82	83	96	96	83	81
Failures	0	0	14	13	0	0	13	15
Rate of success	100%	100%	85%	86%	100%	100%	86%	84%

TABLE I: Number of successfully accomplished tasks. A targeted orientation is considered not reached after an elapsed time of 90s.

3 Contact Points					4 contact Points			
Modality	F+V	F _⊥ +V	F+C	F _⊥ +C	F+V	F _⊥ +V	F+C	F _⊥ +C
Mean [s]	8.64	7.07	32.90	33.41	10.03	9.64	38.11	39.47
STD [s]	5.83	4.36	30.31	29.87	6.24	5.45	25.21	27.37

TABLE II: Mean completion time and standard deviation (STD) for each tested condition.

B. Varying Vibration Intensity (V)

Differently from the previous experiment, in this case the intensity of the motor vibration is regulated proportionally to the actual error in orientation. The motors reference value is computed as in the previous experiment (Section III-A) following (3), (4), and (5). Then, at each time t the i -th motor PWM value is calculated as

$$m_i(t) = \begin{cases} 70 + \alpha(t)|m_i| & \text{if } |m_i| > 0 \\ 0 & \text{otherwise} \end{cases}$$

being

$$\alpha(t) = \frac{\|{}^W\mathbf{R}_O(t)\bar{\mathbf{w}} - \mathbf{g}\|}{2} \cdot 185$$

where ${}^W\mathbf{R}_O$ is the actual hand orientation with respect to the world reference frame (Σ_W), $\bar{\mathbf{w}}$ is the virtual wrench, and $\mathbf{g} = [0 \ 0 \ 1]^T$ is the gravity acceleration expressed in world coordinates.

As in the previous experiment, the trial ends when the error in orientation remains under the threshold for at least 0.5s. Participants performed the test both modeling the grasping with three and four contact points.

Results and discussion are reported in the Section IV.

IV. RESULTS AND DISCUSSION

In this section, we describe and discuss results of the proposed experimental validation. Mean and standard deviation of the time needed by users to orient the hand are reported in Table II. In what follows, we analyze and discuss more in detail results and users' experience feedback comparing the modalities C and V. As a conclusion, results of the statistical analysis and questionnaire answers are reported.

Constant Vibration Intensity Modality (C): In this experiment we examined the human capability in orienting the hand following instructions given without any information about the current error. Twelve trials were repeated using F and F_⊥ conditions, with 3 and 4 contact points. Detailed results are reported in Table I and Table II.

Modality		MD	PD	TD	PE	EF	FR
Constant Intensity	Mean	4.03	1.62	2.51	5.69	4.61	4.83
	STD	1.82	1.08	1.54	1.06	1.79	2.78
Variable Intensity	Mean	3.56	1.58	2.61	2.57	4.42	2.32
	STD	1.96	1.23	1.43	1.60	1.37	1.78

TABLE III: Mean and standard deviation (STD) for the NASA workload questionnaire.

The outcomes of the post execution survey (Table III) revealed that the constant vibration intensity modality is perceived harder and more demanding compared to the varying vibration intensity one. In case of 3 contact points, the success rate was 85% and 86% for the F and F_{\perp} , respectively. Similar results were obtained with 4 contact points where users failed to correctly orient the hand in total 28 times, 13 using the F-policy and 15 with the F_{\perp} one.

Variable Vibration Intensity Modality (V): As in the previous case, we evaluated the task completion time as measure of performance. Twelve trials were carried out with F and F_{\perp} feedback strategies, with 3 and 4 contact points. Detailed results are reported in Table I and Table II. Users' evaluation *a-posteriori* (Table III) reveals that users prefer the variable vibration intensity approach. Moreover, all the participants were able to complete successfully the task, aligning the virtual wrench with the gravity in less than 90 s.

Constant vs Variable Vibration Intensity Modality: A comparison among the two modalities was carried out with a statistical analysis of the data. Since this paper is focused on discriminating the best feedback approach, data were grouped and analyzed by feedback type (F+C, F_{\perp} +C, F+V, and F_{\perp} +V) regardless the number of contact points.

A one-way repeated measures ANOVA was conducted to determine whether there were statistically significant differences between the completion time over the four modalities. There were 7 outliers (4 in F+V, and 3 in F_{\perp} +V) in the data, as assessed by inspection of a boxplot for values greater than 1.5 box-lengths from the edge of the box. These values were removed together with the paired ones without affecting the dataset balancing. It is worth pointing out that we considered outliers cases in which people do not fail the trial, but needed considerably more time to reach the target orientation compared to the task global average.

Data were transformed using the squareroot transformation and passed the ShapiroWilk normality test ($p > 0.05$). The assumption of sphericity was not violated, as assessed by Mauchly's test of sphericity, $\chi^2(5) = 10.56$, $p = 0.061$. The results of the test assessed that the feedback modality elicited statistically significant changes in completion time, $F = 26.759$, $p < 0.0005$. Post hoc analysis with a Bonferroni adjustment revealed that the reduction of time elapsed for orienting the hand was statistically significant. The Bonferroni correction is used to reduce the possible false positive results when multiple pair-wise tests are performed. More in detail, the difference between F_{\perp} +C and F_{\perp} +V was 26.34 s,

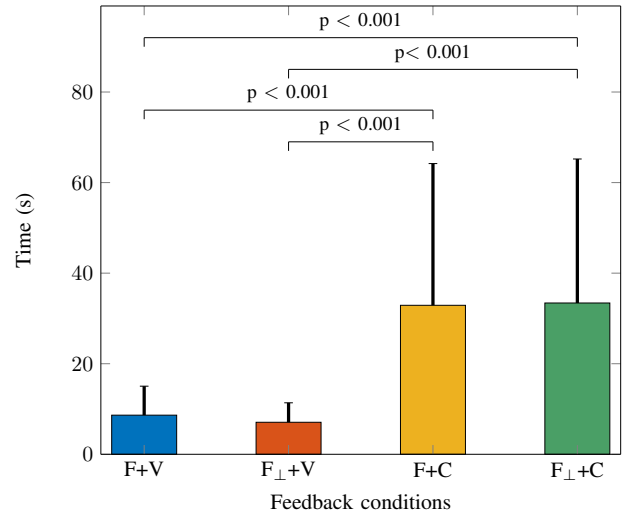


Fig. 4: Experimental Validation results. Mean and standard deviation of the four feedback conditions are plotted. The p-values, computed with one-way repeated measures ANOVA, are reported above the bar charts.

while the average reduction time from F_{\perp} +C to F+V was 24.77 s. For what concerns F+C, we observed a difference of 24.25 s with F_{\perp} +V and 25.83 s with F+V. On the other hand, the one-way repeated measure ANOVA revealed no statistically significant difference between F+C and F_{\perp} +C, F+V and F_{\perp} +V. We assessed thorough the software G*Power that considered values from the 8 participants are enough for having a power of 0.80. Results are graphically depicted in Figure 4.

Concerning the perceived workload demanded by our guidance policies, the results of the questionnaires are reported in Table III and lead to the following conclusions. The frustration (FR) in following the haptic suggestion was evaluated very low for the Variable feedback (2.32 ± 1.78) while it was higher for Constant feedback (4.83 ± 2.78). The effort (EF) was rated equal in both cases (4.61 ± 1.79 and 4.42 ± 1.37 for C and V, respectively). Participants judge the performance (PE) of C and V remarkably different (for this question the lower the score the better the perception of success). User perception is in line with numerical results. In fact, the score (5.69 ± 1.06) is associated with a high number of failures in orienting the hand (the average success rate is 85%). On the other hand, participants considered close to the perfection the accomplishment in V. The temporal and physical demand (TD and PD) scored a low effort demanding, whereas the mental demand (MD) was rated a bit higher than the previous two, but we can consider 4.03 ± 1.82 and 3.56 ± 1.92 acceptable values, given the proprieties of our guiding system.

V. CONCLUSION AND FUTURE WORK

In this work, we present an innovative and effective haptic hand guidance system. We use vibrotactile thimbles for suggesting hand orientation, implementing a grasping

metaphor. The system has been validated with user experiments aimed to test if participants were able to orient the hand as requested. Two different feedback strategies have been proposed. Results, supported by the statistical analysis, show that to give information about the actual orientation is crucial to accomplish the task in minor time. Beside the quantitative results, users' opinion points out an evident preference for this policy. As far as it concerns the technological aspect, the use of thimble-factor devices guarantees high portability and wearability of the system, it reduces power consumption increasing the battery lifetime. The main novelties that our approach introduces with respect to the currently available solutions can be summarized as follows: *i*) the hand is directly controlled displaying cues in the most sensitive location [26]; *ii*) no encumbering devices prevent the user's hand to be free; *iii*) the hand orientation is suggested independently from other body parts, increasing the haptic guidance capability; *iv*) human arm singularities are avoided by charging the inverse kinematics computation to the brain instead of to an algorithm; *v*) the approach can be combined with any hand tracking system, like camera-based (Vicon, Optitrack, LeapMotion), inertial-based ([27], [28]) and fabric-based (Cyberglove) devices. In conclusion, we believe that the proposed system paved the way for the development of more complex systems. Virtual Reality, teleoperation, rehabilitation, and training are representative scenarios in which this approach can be adopted. Wearable haptic interface with different feedback modalities (pressure, skin stretch, etc.) can be used for enriching the conveyed information, thus having a more immersive system. Further studies will be aimed to investigate more in detail the difference between multiple contact points strategies. Moreover, since in this proof of concept stage we discard rotation around the gravity axes (the z axis in this manuscript) in future work we plan to add vibrational patterns to encode the missing orientation cue.

REFERENCES

- [1] G. Spagnoletti, L. Meli, T. Lisini Baldi, G. Gioioso, C. Pacchierotti, and D. Prattichizzo, "Rendering of pressure and textures using wearable haptics in immersive vr environments," in *Proc. IEEE Virtual Reality*. IEEE, 2018, pp. 691–692.
- [2] D. Prattichizzo, F. Chinello, C. Pacchierotti, and M. Malvezzi, "Towards wearability in fingertip haptics: a 3-dof wearable device for cutaneous force feedback," *IEEE Trans. Haptics*, vol. 6, no. 4, pp. 506–516, 2013.
- [3] I. Karuei and K. E. MacLean, "Susceptibility to periodic vibrotactile guidance of human cadence," in *Proc. IEEE Int. Symp. in Haptic Interfaces for Virtual Environment and Teleoperator Systems*. IEEE, 2014, pp. 141–146.
- [4] T. Lisini Baldi, S. Scheggi, M. Aggravi, and D. Prattichizzo, "Haptic guidance in dynamic environments using optimal reciprocal collision avoidance," *IEEE Robotics and Automation Letters*, vol. 3, no. 1, pp. 265–272, 2017.
- [5] M. Aggravi, G. Salvietti, and D. Prattichizzo, "Haptic wrist guidance using vibrations for human-robot teams," in *Proc. IEEE Int. Symp. in Robot and Human Interactive Communication*. IEEE, 2016, pp. 113–118.
- [6] D. Feygin, M. Keehner, and R. Tendick, "Haptic guidance: Experimental evaluation of a haptic training method for a perceptual motor skill," in *Proc. IEEE Int. Symp. in Haptic Interfaces for Virtual Environment and Teleoperator Systems*. IEEE, 2002, pp. 40–47.
- [7] W. Guo, W. Ni, I.-M. Chen, Z. Q. Ding, and S. H. Yeo, "Intuitive vibro-tactile feedback for human body movement guidance," in *Proc IEEE Int. Conf on Robotics and Biomimetics*. IEEE, 2009, pp. 135–140.
- [8] A. M. Okamura, "Methods for haptic feedback in teleoperated robot-assisted surgery," *Industrial Robot: An International Journal*, vol. 31, no. 6, pp. 499–508, 2004.
- [9] S. Schätzle, T. Hulin, C. Preusche, and G. Hirzinger, "Evaluation of vibrotactile feedback to the human arm," in *Proc. of Eurohaptics Conference*, 2006, pp. 557–560.
- [10] B. Weber, S. Schätzle, T. Hulin, C. Preusche, and B. Deml, "Evaluation of a vibrotactile feedback device for spatial guidance," in *Proc. IEEE World Haptics Conference*. IEEE, 2011, pp. 349–354.
- [11] E. P. Westebring-van der Putten, R. H. Goossens, J. J. Jakimowicz, and J. Dankelman, "Haptics in minimally invasive surgery—a review," *Minimally Invasive Therapy & Allied Technologies*, vol. 17, no. 1, pp. 3–16, 2008.
- [12] T. Dyrks, S. Denef, and L. Ramirez, "An empirical study of firefighting sensemaking practices to inform the design of ubicomp technology," in *Proc. ACM Int. Conf. on Human Factors in Computing Systems*, 2008.
- [13] T. Amemiya, H. Ando, and T. Maeda, "Lead-me interface for a pulling sensation from hand-held devices," *ACM Transactions on Applied Perception*, vol. 5, no. 3, p. 15, 2008.
- [14] J. M. Walker, H. Culbertson, M. Raitor, and A. M. Okamura, "Haptic orientation guidance using two parallel double-gimbal control moment gyroscopes," *IEEE Trans. Haptics*, vol. 11, no. 2, pp. 267–278, 2017.
- [15] A. Spiers, A. Dollar, J. Van Der Linden, and M. Oshodi, "First validation of the haptic sandwich: A shape changing handheld haptic navigation aid," in *Proc. IEEE Int. Conf. on Advanced Robotics*. IEEE, 2015, pp. 144–151.
- [16] F. Chinello, C. Pacchierotti, J. Bimbo, N. G. Tsarakakis, and D. Prattichizzo, "Design and evaluation of a wearable skin stretch device for haptic guidance," *IEEE Robotics and Automation Letters*, vol. 3, no. 1, pp. 524–531, 2017.
- [17] T. Oron-Gilad, J. L. Downs, R. D. Gilson, and P. A. Hancock, "Vibrotactile guidance cues for target acquisition," *IEEE Transactions on Systems, Man, and Cybernetics, Part C (Applications and Reviews)*, vol. 37, no. 5, pp. 993–1004, 2007.
- [18] J. Reimer, "A history of the gui," *Ars Technica*, vol. 5, pp. 1–17, 2005.
- [19] C. Pacchierotti, S. Sinclair, M. Solazzi, A. Frisoli, V. Hayward, and D. Prattichizzo, "Wearable haptic systems for the fingertip and the hand: taxonomy, review, and perspectives," *IEEE Trans. Haptics*, vol. 10, no. 4, pp. 580–600, 2017.
- [20] D. Prattichizzo and J. C. Trinkle, "Grasping," *Springer handbook of robotics*, pp. 671–700, 2008.
- [21] G. Baud-Bovy, D. Prattichizzo, and N. Brogi, "Does torque minimization yield a stable human grasp?" in *Multi-point Interaction with Real and Virtual Objects*. Springer, 2005, pp. 21–40.
- [22] S. Boyd and L. Vandenberghe, *Convex optimization*. Cambridge university press, 2004.
- [23] "Precision microdrives 10mm vibration motor model: 310-103 product data sheet." [Online]. Available: <https://www.precisionmicrodrives.com/product/datasheet/310-103-10mm-vibration-motor-3mm-type-datasheet.pdf>
- [24] H. Z. Tan, M. A. Srinivasan, C. M. Reed, and N. I. Durlach, "Discrimination and identification of finger joint-angle position using active motion," *ACM Transactions on Applied Perception*, vol. 4, no. 2, p. 10, 2007.
- [25] S. G. Hart, "Nasa-task load index (nasa-tlx); 20 years later," in *Proceedings of the human factors and ergonomics society annual meeting*, vol. 50, no. 9. Sage publications Sage CA: Los Angeles, CA, 2006, pp. 904–908.
- [26] C. Gaudeni, L. Meli, L. Jones, and D. Prattichizzo, "Presenting surface features using a haptic ring: A psychophysical study on relocating vibrotactile feedback," *IEEE Trans. Haptics*, 2019.
- [27] T. Lisini Baldi, S. Scheggi, L. Meli, M. Mohammadi, and D. Prattichizzo, "GESTO: A glove for enhanced sensing and touching based on inertial and magnetic sensors for hand tracking and cutaneous feedback," *IEEE Trans. Human-Mach. Syst.*, vol. 47, no. 6, pp. 1066–1076, 2017.
- [28] H. G. Kortier, V. I. Sluiter, D. Roetenberg, and P. H. Veltink, "Assessment of hand kinematics using inertial and magnetic sensors," *Journal of Neuroengineering and Rehabilitation*, vol. 11, no. 1, p. 70, 2014.